Somatostatin Receptor 1 Selective Analogues: 2. N^{α}-Methylated Scan†

Judit Erchegyi,‡ Carl A. Hoeger,‡ William Low,‡ Daniel Hoyer,§ Beatrice Waser,|| Véronique Eltschinger,|| Jean-Claude Schaer,|| Renzo Cescato,|| Jean Claude Reubi,|| and Jean E. Rivier*,‡

The Clayton Foundation Laboratories for Peptide Biology, The Salk Institute, 10010 North Torrey Pines Road, La Jolla, California, 92037, Neuroscience Research, Novartis Institutes for Biomedical Research, Novartis Pharma AG, Basel, Switzerland, and Division of Cell Biology and Experimental Cancer Research, Institute of Pathology, University of Berne, Berne, Switzerland

Received June 18, 2004

Des-$AA^{1,2,5}$-[D-Trp^8/D-Nal^8,$IAmp^9$]SRIF (AA = amino acid, Nal = 3-(2-naphthyl)-alanine, IAmp = 4-(*N*-isopropyl)-aminomethylphenylalanine, SRIF = somatostatin), with or without a tyrosine or monoiodotyrosine, were scanned with the introduction of a backbone *N*-methyl group and tested for binding affinity at the five human somatostatin receptors (sst_{1-5}). N^{α}-Methylation resulted in loss of sst affinity (2- to >5-fold) when introduced at residues Lys^4 (**6**), Phe^6 (**7**), Phe^7 (**8**), Thr^{10} (**11**), and Phe^{11} (**12**) of the parent compound Des-$AA^{1,2,5}$-[D-Nal^8,$IAmp^9$]SRIF (**4**). N^{α}-Methylation was tolerated at residues Cys^3 (**5**), D-Nal^8 (**9**), Thr^{12} (**13**), and Cys^{14} (**15**) with retention of binding sst affinity and selectivity and resulted in an increase in sst binding affinity at positions $IAmp^9$ (**10**) and Ser^{13} (**14**). In these series, the D-Trp^8 substitution versus D-Nal^8 is clearly superior. C-Terminally lysine-extended analogues (**21**−**25**) retained sst_1 selectivity and binding affinity when compared to their D-Nal^8- (**4**) or D-Trp^8- (**3**) containing parent. Des-$AA^{1,2,5}$-[D-Trp^8, (N^{α}Me)$IAmp^9$]SRIF (**17**), Des-$AA^{1,2,5}$-[D-Trp^8,$IAmp^9$,(N^{α}Me)Ser^{13}]-SRIF (**19**), Des-$AA^{1,2,5}$-[D-Trp^8,$IAmp^9$,(N^{α}Me)Cys^{14}]SRIF (**20**), Des-$AA^{1,2,5}$-[D-Trp^8,(N^{α}Me)$IAmp^9$,-Tyr^{11}]SRIF (**34**), and Des-$AA^{1,2,5}$-[D-Agl^8(N^{β}Me,2-naphthoyl),$IAmp^9$,Tyr^{11}]SRIF (**42**) (Agl = aminoglycine) are sst_1 agonists in their ability to inhibit forskolin-induced cAMP production.

Introduction

Somatostatin (SRIF) is a major endocrine hormone and physiological inhibitor of growth hormone (GH),[3] glucagon, and insulin secretion.[4] With the characterization of five somatostatin receptors in the early 1990s,[5−11] cell lines bearing these cloned receptor subtypes (sst) are now available to test SRIF analogues for binding affinity, selectivity, and function.[12,13] Consequently, in the clinic, such a broadly used analogue as octreotide[14] is now recognized as unequally potent at the different receptors.[15−17] Because only a few functions have so far been assigned to each receptor for lack of selective ligands (agonists and antagonists), the search continues for receptor ligands, peptidic or nonpeptidic in nature with high affinity and selectivity for the identified receptors.

Sst_1 receptor has been found in human cerebral cortex,[18] human tumors,[19] neuroblastoma,[20] "nonfunctioning" pituitary adenomas,[21] cervical carcinoma and endometrial carcinoma,[22] human retina,[23] glioblastoma multiform,[24] and neuroendocrine cells.[25] According to Lanneau[26] and Olias,[25] sst_1 receptors are involved in the intrahypothalamic regulation of GH secretion. An important role for hypothalamic sst_1 in the sexual dimorphism of GH secretion was also suggested.[25,27] Similarly, activation of sst_1 may selectively inhibit GH and prolactin secretion from human pituitary adenomas.[28] It was suggested that more selective analogues are needed to establish the role of sst_1 in hypothalamic glutamate currents.[13] Sst_1 receptor also modulates somatostatin release in basal ganglia.[29] Recently, an sst_1 antagonist was shown to promote social interactions, reduce aggressive behavior, and stimulate learning.[30,31] Sst_1 also functions as an autoreceptor in the retina, so sst_1-selective analogues could play an important role in retinal disease therapeutics.[23]

In summary, there is still a need for further refinements in the localization and physiological functions of sst_1, and the design of more potent sst_1-selective analogues can fulfill this need both in vitro and in vivo.

Although SRIF itself may be administered to patients, its use is still limited by its short duration of action as compared to that of SRIF analogues such as octreotide, lanreotide, and vapreotide[32] that offer some selectivity and extended duration of action. Structurally, all of these analogues are similar in that they are 18-atom cycles with single amino acids appended at both the N- and C-termini. All of these analogues tend to be selective for sst_2, sst_3, and sst_5 to a lesser extent. We have identified a different scaffold (Des-$AA^{1,2,5}$-SRIF) (AA= amino acid, SRIF = somatostatin) that in combination with a D-Trp residue at position 8 and a 4-(*N*-isopropyl)-aminomethylphenylalanine (IAmp) residue at position 9 yields SRIF agonists that are sst_1-selective.[1,2,33] An aromatic D amino acid at position 8 such as D-Trp^8 or D-Nal^8 (Nal = 3-(2-naphthyl)-alanine) increases the potency of SRIF analogues,[34−37] yet, we have recently shown that this configuration is deleterious in the design of sst_4-selective analogues.[38,39]

Several biological studies have been carried out using sst_1-selective analogues that allow identification of both

* Author to whom correspondence should be addressed. Phone: (858) 453-4100. Fax: (858) 552-1546. E-mail: Jrivier@salk.edu.

† Part 1 is ref 1. This work was presented in part at the 17th American Peptide Symposium.[2]

‡ The Salk Institute.

§ Novartis Pharma AG.

|| University of Berne.

10.1021/jm049520l CCC: $30.25
Published on Web 12/23/2004

localization[40] and limited functions for this receptor.[20] An sst_1-selective nonpeptide ligand L-797,591 has also been described.[41]

Whereas we have already described the synthesis of Des-AA^{1,2,5}-[D-Trp^8,IAmp^9,Tyr^{11}]SRIF **(32)** as an sst_1-selective agonist amenable to ^{125}I labeling with retention of high-binding affinity (IC_{50} = 3.6 nM at sst_1 and IC_{50} >1000 at the other four sst) for tissue labeling,[1] our search continues for sst_1-selective antagonists as well as for sst_1-selective ligands with structural constraints in order to define those structural parameters responsible for sst_1 selectivity.

We present here the effect of additional structural modifications (N^α-methylation of the backbone and tyrosine substitutions) of the general scaffold represented by Des-AA^{1,2,5}-[D-Nal^8/D-Trp^8,IAmp^9]SRIF[1] on binding affinities and selectivities for the five human SRIF receptors (sst). It should be noted that a similar scan of two octapeptide agonists cyclo(6,11)[H-D-Phe^5-and Tyr^5-Cys^6-Phe^7-D-Trp^8-Lys^9-Thr^{10}-Cys^{11}-Thr^{12}-NH_2][42] and one antagonist cyclo(6,11)[H-Cpa^5-D-Cys^6-Pal^7-D-Trp^8-Lys^9-Thr^{10}-Cys^{11}-Nal^{12}-NH_2][43] of SRIF have been reported. Although results emphasize the unpredictability of the introduction of such constraints on both affinity and selectivity, there was consensus that N^α-methylation of the residue corresponding to Lys^9 in somatostatin resulted in either maintenance or increase of affinity. N^α-Methylation at other positions resulted in loss of affinity or some subtle modulation of selectivity. In part 3,[44] we describe the effect of the introduction of a second bridge in the parent Des-AA^{1,2,5}-[D-Trp^8,IAmp^9,Tyr^{11}]SRIF (**32**) on sst_1 selectivity and binding affinity, and in part 4 we describe a three-dimensional consensus structure of sst_1-selective analogues derived from NMR studies.[45]

Results and Discussion

Peptide Synthesis. All of the analogues shown in Table 1 were synthesized either manually or automatically on a chloromethylated resin using the Boc (*t*-butoxycarbonyl) strategy and *N*,*N*′-diisopropylcarbodiimide (DIC) for amide bond formation. N^α-Methylation of the backbone was achieved on the resin using the method of Kaljuste.[46] This approach was successful and used for the synthesis of all of the N^α-methylated analogues in Table 1, with the exception of **15**, **19**, and **20**. Indeed, we were not able to methylate Cys^{14} of **15** on the resin using this method. An alternative was to use the method described by Miller et al. (Experimental Section).[47] This attempt also proved to be unsuccessful. Steric hindrance most likely caused the poor reactivity of the nitrogens at or near the C-terminus, as it was observed by others.[42] This is exemplified by the successful (yet with very low yields) N^α-methylation of serine at position 13 in **14**. Therefore, on the basis of the premise that failure to achieve methylation was due to proximity of the residue to be methylated to the resin, we introduced two (**21**) or three (**22**, **24**) lysine residues at the C-terminus of the desired peptides. We hypothesized that the lysine residues would extend the peptide chain in such a way that C-terminal steric interferences would disappear. First, we found that the elongated peptides were suitable for methylation of the first or second residue beyond the lysines on the resin using the method of Kaljuste.[46] Second, we found that the enzymatic hydrolysis of the two or three lysine-elongated purified peptides using a carboxypeptidase B enzyme preparation ultimately yielded the desired analogues in good yields. This enzyme is well-known to catalyze the hydrolysis of the peptide bond liberating the C-terminal amino acid of a peptide chain when this amino acid is arginine, lysine, or ornithine.[48] Interestingly, we first isolated the desired peptide C-terminally extended with one lysine (**23**, **25**) and only with exhaustive enzymatic treatment the desired, non-lysine-containing analogues (**15**, **19**, **20**). For the synthesis of N^αMe-IAmp-containing analogues (**27**, **29**, **30**, **34**, **35**, **37**, and **39**−**41**), we prepared Boc-N^αMe-IAmp(Z) in solution and used it in the solid-phase synthesis.

The peptide resins were treated with hydrogen fluoride in the presence of scavengers to liberate the fully deblocked crude peptides. Cyclization of the cysteines was mediated by iodine in an acidic milieu or by the potassium ferricyanide method.[49] The iodine oxidation procedure was preferred because it does not require the ion-exchange step necessary to eliminate the ferri- or ferrocyanide salts. Purification was carried out using multiple high-performance liquid chromatography (HPLC) steps,[50] and characterization was carried out by HPLC,[50] capillary zone electrophoresis,[51] and mass spectrometry. The C-terminus-extended purified target peptides (**21**, **22**, and **24**) could be hydrolyzed with carboxypeptidase B resulting in the desired analogues (**15**, **19**, and **20**). Additionally, the relatively slow kinetics of hydrolysis of the third lysines in **22** and **24** followed by HPLC allowed the isolation of **23** and **25** in good yields. The measured masses obtained using MALDI-MS were within 100 ppm of those calculated for the protonated molecule ions.

Biological Testing. The compounds were tested for their ability to bind to 20 μm thick cryostat (Leitz 1720, Rockleigh, NJ) sections of a membrane pellet of cells transfected with the five human sst receptor subtypes. For each of the tested compounds, complete displacement experiments with the universal SRIF radioligand [Leu^8,D-Trp^{22},^{125}I-Tyr^{25}]SRIF-28 using increasing concentrations of the unlabeled peptide ranging from 0.1 to 1000 nM were performed. The unlabeled SRIF-28 was run in parallel using the same increasing concentrations as control (SRIF-28 = somatostatin-28). IC_{50} values were calculated after quantification of the data using a computer-assisted image processing system as described previously.[19,52] Tissue standards (Autoradiographic [^{125}I] microscales, Amersham) that contain known amounts of isotope, cross calibrated to tissue-equivalent ligand concentrations, were used for quantitation.[53] Advantages of the present method using receptor autoradiography with sectioned cell pellets compared to binding on cell homogenates are, in addition to an economy on cells and a great flexibility, the greater interassay reliability and reproducibility, because sections of the same embedded pellet can be used for successive experiments. As a minor disadvantage, IC_{50} values are somewhat higher than those in the homogenate binding assay.[52] Potent or receptor-selective analogues selected for their chemical diversity were then evaluated for their agonist/antagonist properties measuring the forskolin-stimulated production of cyclic adenosine monophos-

Table 1. Effect of Backbone Methylation on Potency and Selectivity of CH-275 and Analogues[e]

	compound	HPLC[a]	CZE[b]	MS[c] M calc.	MS[c] $[M+H]^+$	IC_{50} (nM)[d] sst_1	sst_2	sst_3	sst_4	sst_5
1	SRIF-28	>98	>98	3146.48	3147.3	3.2 ± 0.2 (38)	2.3 ± 0.1 (39)	3.7 ± 0.3 (38)	2.6 ± 0.1 (37)	2.4 ± 0.2 (36)
2*	Des-AA^5-[D-Trp^8]SRIF	98	97	1522.67	1523.2	0.98 (0.75, 1.2)	43 (40, 45)	3.4 (3.6, 3.1)	1.7 (1.3, 2.0)	5.0 (4.0, 6.0)
3*	Des-AA^{1,2,5}-[D-Trp^8,IAmp^9]SRIF CH-275	94	97	1484.66	1485.5	33 ± 10 (3)	>1K (2)	345 (540, 150)	>1 K (2)	>1 K (2)
4	Des-AA^{1,2,5}-[D-Nal^8,IAmp^9]SRIF	97	>98	1495.68	1496.6	248 ± 168 (3)	>1K (3)	>1K (2)	>1 K (2)	>1 K (2)
5	Des-AA^{1,2,5}-[(N^{α}Me)Cys^3,D-Nal^8,IAmp^9]SRIF	89	98	1509.69	1510.8	113 (26, 200)	> 1K (2)	> 1K (2)	>1 K (2)	>1 K (2)
6	Des-AA^{1,2,5}-[(N^{α}Me)Lys^4,D-Nal^8,IAmp^9]SRIF	98	96	1509.69	1510.7	535 (420, 650)	> 1K (2)	> 1K (2)	>1 K (2)	>1 K (2)
7	Des-AA^{1,2,5}-[(N^{α}Me)Phe^6,D-Nal^8,IAmp^9]SRIF	90	92	1509.69	1510.7	>1 K (3)	> 1K (3)	> 1K (2)	>1 K (2)	>1 K (2)
8	Des-AA^{1,2,5}-[(N^{α}Me)Phe^7,D-Nal^8,IAmp^9]SRIF	98	>98	1509.69	1510.8	>1 K (2)	> 1K (2)	> 1K (2)	>1 K (2)	>1 K (2)
9	Des-AA^{1,2,5}-[(N^{α}Me)D-Nal^8,IAmp^9]SRIF	97	>98	1509.69	1510.7	325 (190, 460)	>1K (2)	> 1K (2)	>1 K (2)	>1 K (2)
10	Des-AA^{1,2,5}-[D-Nal^8,(N^{α}Me)IAmp^9]SRIF	>98	>98	1509.69	1510.8	69 ± 29	>1 K (2)	>1 K (2)	>1 K (2)	>1 K (2)
11	Des-AA^{1,2,5}-[D-Nal^8,IAmp^9,(N^{α}Me)Thr^{10}]SRIF	97	97	1509.69	1510.8	>1 K (2)	>1 K (3)	>1 K (2)	>1 K (2)	>1 K (2)
12	Des-AA^{1,2,5}-[D-Nal^8,IAmp^9,(N^{α}Me)Phe^{11}]SRIF	95	95	1509.69	1510.6	583 (620, 546)	>1 K (3)	> 1 K (3)	>1 K (2)	>1 K (2)
13	Des-AA^{1,2,5}-[D-Nal^8,IAmp^9,(N^{α}Me)Thr^{12}]SRIF	>98	95	1509.69	1510.6	176 (170, 182)	>1 K (2)	> 1 K (2)	417 (400, 433)	>1 K (2)
14	Des-AA^{1,2,5}-[D-Nal^8,IAmp^9,(N^{α}Me)Ser^{13}]SRIF	93	97	1509.69	1510.5	71 ± 14 (4)	>1 K (3)	> 1 K (3)	>1 K (3)	>1 K (3)
15	Des-AA^{1,2,5}-[D-Nal^8,IAmp^9,(N^{α}Me)Cys^{14}]SRIF	>98	98	1509.69	1510.7	260 (290, 229)	>1 K (2)	>1 K (2)	>1 K (2)	>1 K (2)
16	Des-AA^{1,2,5}-[(N^{α}Me)Cys^3,D-Trp^8,IAmp^9]SRIF	95	97	1498.68	1499.5	14 ± 3 (3)	>1 K (3)	>1 K (3)	>1 K (3)	>1 K (3)
17	Des-AA^{1,2,5}-[D-Trp^8,(N^{α}Me)IAmp^9]SRIF	97	>98	1498.68	1499.8	10 (8.7, 12)	>1 K (2)	1029 (610, 1447)	226 (200, 252)	>1 K (2)
18	Des-AA^{1,2,5}-[D-Trp^8,IAmp^9,(N^{α}Me)Thr^{12}]SRIF	>98	>98	1498.68	1499.8	75 (70, 79)	>1 K (2)	>1 K (2)	>1 K (2)	>1 K (2)
19	Des-AA^{1,2,5}-[D-Trp^8,IAmp^9,(N^{α}Me)Ser^{13}]SRIF	98	98	1498.68	1499.8	23 (25, 21)	>1 K (2)	>1 K (2)	>1 K (2)	>1 K (2)
20	Des-AA^{1,2,5}-[D-Trp^8,IAmp^9,(N^{α}Me)Cys^{14}]SRIF	90	97	1498.68	1499.8	151 (160, 142)	>1 K (2)	>1 K (2)	>1 K (2)	>1 K (2)
21	Des-AA^{1,2,5}-[D-Trp^8,IAmp^9,(N^{α}Me)Ser^{13}]SRIF−$(Lys)_2$	98	96	1754.87	1756.0	53 (46, 60)	>1 K (2)	> 1K (2)	>1 K (2)	682 (800, 563)
22	Des-AA^{1,2,5}-[D-Nal^8,IAmp^9,(N^{α}Me)Cys^{14}]SRIF−$(Lys)_3$	>98	98	1893.97	1895.1	144 (170, 118)	>1 K (2)	620 (500, 739)	>1 K (2)	>1 K (2)
23	Des-AA^{1,2,5}-[D-Nal^8,IAmp^9,(N^{α}Me)Cys^{14}]SRIF−Lys	>98	>98	1637.79	1638.2	255 (230, 280)	>1 K (2)	> 1K (2)	>1 K (2)	> 1K (2)
24	Des-AA^{1,2,5}-[D-Trp^8,IAmp^9,(N^{α}Me)Cys^{14}]SRIF−$(Lys)_3$	97	85	1882.96	1884.0	30 (35, 24)	>1 K (2)	>1 K (850, 1500)	>1 K (2)	803 (750, 855)
25	Des-AA^{1,2,5}-[D-Trp^8,IAmp^9,(N^{α}Me)Cys^{14}]SRIF−Lys	95	82	1626.77	1627.8	35 (40, 29)	> 1K (2)	>1 K (2)	>1 K (2)	> 1K (2)
26*	Des-AA1,5-[Tyr^2,D-Trp^8,IAmp^9]SRIF CH-288	96	98	1184.48	1185.5	14 ± 2.7 (8)	>1 K (6)	>1 K (6)	>1 K (6)	>1 K (7)
27	Des-AA1,5-[Tyr^2,D-Trp^8,(N^{α}Me)IAmp^9]SRIF	95	>98	1661.74	1662.7	16 (25, 6.5)	>1 K (2)	> 1K (2)	245 (300, 189)	>1 K (2)
28*	Des-AA1,5-[Tyr^2,D-Trp^8,IAmp^9]Cbm-SRIF	94	98	1690.73	1691.8	15 ± 4 (3)	> 1K (3)	500 ± 50 (3)	>1 K (3)	>1 K (3)
29	Des-AA1,5-[Tyr^2,D-Trp^8,(N^{α}Me)IAmp^9]Cbm-SRIF	95	98	1704.75	1705.9	45 (68, 22)	> 1K (2)	>1 K (2)	418 (450, 385)	>1 K (2)
30	Des-AA1,5-[m-I-Tyr^2,D-Trp^8,(N^{α}Me)IAmp^9]Cbm-SRIF	87	94	1830.64	1831.8	43 (60, 26)	> 1K (2)	>1 K (2)	772 (850, 693)	> 1K (2)
31	Des-AA^{1,2,5}-[D-Trp^8,Tyr^{11}]SRIF	99	98	1094.44	1095.3	10 ± 1 (3)	16 ± 6 (3)	8 ± 4 (3)	0.5 ± 0.09 (3)	4.8 ± 0.3 (3)
32*	Des-AA^{1,2,5}-[D-Trp^8,IAmp^9,Tyr^{11}]SRIF [Tyr^{11}]CH-275	98	96	1500.66	1501.5	17 ± 6 (5)	>1 K (5)	>1 K (5)	> 1K (5)	> 1K (5)
33	Des-AA^{1,2,5}-[IAmp^9,Tyr^{11}]SRIF	>98	>98	1500.66	1501.5	15 (18, 11)	>1 K (2)	>1K (2)	384 (360, 408)	>1K (2)
34	Des-AA^{1,2,5}-[D-Trp^8,(N^{α}Me)IAmp^9,Tyr^{11}]SRIF	>98	>98	1514.68	1515.6	7.2 (6.1, 8.2)	>1 K (2)	>1 K (2)	>1 K (2)	>1 K (2)
35	Des-AA^{1,2,5}-[D-Trp^8,(N^{α}Me)IAmp^9,m-I-Tyr^{11}]SRIF	>98	>98	1640.57	1641.6	5.2 (7.3, 3.1)	>1 K (2)	>1 K (2)	>1 K (2)	>1 K (2)
36*	Des-AA^{1,2,5}-[D-Trp^8,IAmp^9,Tyr^{11}]Cbm-SRIF	98	98	1543.66	1544.6	8 ± 1 (5)	>1 K (5)	>1 K (5)	>1 K (5)	>1 K (5)
37	Des-AA^{1,2,5}-[D-Trp^8,(N^{α}Me)IAmp^9,Tyr^{11}]Cbm-SRIF	98	>98	1557.69	1558.7	5.8 (4.2, 7.3)	>1 K (2)	311 (328, 293)	>1 K (2)	>1 K (2)
38*	Des-AA^{1,2,5}-[D-Trp^8,IAmp^9,m-I-Tyr^{11}]Cbm-SRIF	91	97	1669.57	1670.6	2.5 ± 0.2 (4)	> 1K (4)	617 ± 125 (4)	>1 K (4)	>1 K (4)
39	Des-AA^{1,2,5}-[D-Trp^8,(N^{α}Me)IAmp^9,m-I-Tyr^{11}]Cbm-SRIF	90	98	1683.59	1684.6	8.5 ± 2 (3)	>1 K (3)	>1 K (3)	700 ± 126 (3)	> 1K (3)
40	Des-AA^{1,2,5}-[D-Nal^8,(N^{α}Me)IAmp^9,Tyr^{11}]SRIF	96	96	1525.69	1526.6	25 (21, 28)	>1 K (2)	>1 K (2)	>1 K (2)	>1 K (2)
41	Des-AA^{1,2,5}-[D-Nal^8,(N^{α}Me)IAmp^9,Tyr^{11}]Cbm-SRIF	95	97	1568.69	1569.6	22 (32, 11)	>1 K (2)	>1 K (2)	>1 K (2)	>1 K (2)
42	Des-AA^{1,2,5}-[D-Agl^8(N^{β}Me,2-naphthoyl),IAmp^9,Tyr^{11}]SRIF	89	93	1554.67	1555.7	3.3 ± 1 (3)	>1 K (3)	>1 K (3)	562 ± 135 (3)	>1 K (3)
43	Des-AA^{1,2,5}-[L-Agl^8(N^{β}Me,2-naphthoyl),IAmp^9, Tyr^{11}]SRIF	95	91	1554.67	1555.3	>1 K	>1 K	900	>1 K	>1 K
44	Des-AA^{1,2,5}-[D-Agl^8(N^{β}Me,2-naphthoyl),IAmp^9, m-I-Tyr^{11}]SRIF	97	98	1680.56	1681.5	6.7 (7.3, 6.1)	> 1K (2)	536 (698, 374)	435 (442, 428)	> 1K (2)
45	Des-AA^{1,2,5}-[D-Agl^8(N^{β}Me,2-naphthoyl),IAmp^9, m-I-Tyr^{11}]Cbm-SRIF	90	97	1724.58	1725.4	4.8 (6.0, 3.6)	> 1K (2)	953 (1062, 843)	660 (552, 768)	> 1K (2)

[a] Percent purity determined by HPLC using buffer system: A = TEAP (pH 2.5) and B = 60% CH_3CN/40% A with a gradient slope of 1% B/min, at flow rate of 0.2 mL/min on a Vydac C_{18} column (0.21 cm × 15 cm, 5-μm particle size, 300 Å pore size). Detection at 214 nm. [b] Capillary zone electrophoresis (CZE) was done using a Beckman P/ACE System 2050 controlled by an IBM Personal System/2 model 50Z and using a ChromJet integrator. Field strength of 15 kV at 30 °C. Mobile phase: 100 mM sodium phosphate (85:15, H_2O/CH_3CN) pH 2.50, on a Supelco P175 capillary (363 μm o.d. × 75 μm i.d. × 50 cm length). Detection at 214 nm. [c] The calculated *m/z* of the monoisotope compared with the observed $[M+H]^+$ monoisotopic mass. [d] The IC_{50} values (nM) were derived from competitive radioligand displacement assays reflect the affinities of the analogues for the cloned somatostatin receptors using the nonselective [Leu^8,D-Trp^{22},^{125}I-Tyr^{25}]SRIF-28, as the radioligand. Mean value ± SEM when $N \geq 3$ (shown in parentheses). Otherwise, mean with single values in parentheses. [e] SRIF = H-Ala^1-Gly^2-c[Cys^3-Lys^4-Asn^5-Phe^6-Phe^7-Trp^8-Lys^9-Thr^{10}-Phe^{11}-Thr^{12}-Ser^{13}-Cys^{14}]-OH. * Described in part 1, reference 1.

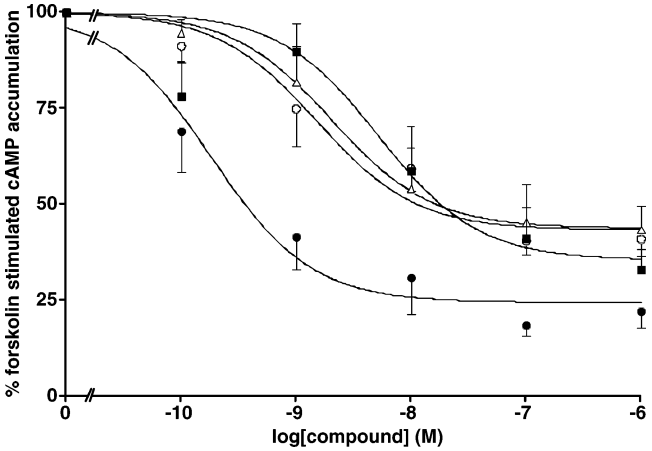

Figure 1. Effect of various concentrations of the sst_1-selective agonists **(17, 19, 42)** in comparison with SRIF-28 as positive control on forskolin-stimulated cAMP accumulation in CCL39 cells expressing sst_1. Concentration−response curves were obtained with increasing concentrations of SRIF-28 (●), **17** (■), **19** (△), and **42** (○). Data are expressed as % forskolin-stimulated cAMP accumulation. The plot represents the mean of three independent experiments in triplicate (mean ± SEM).

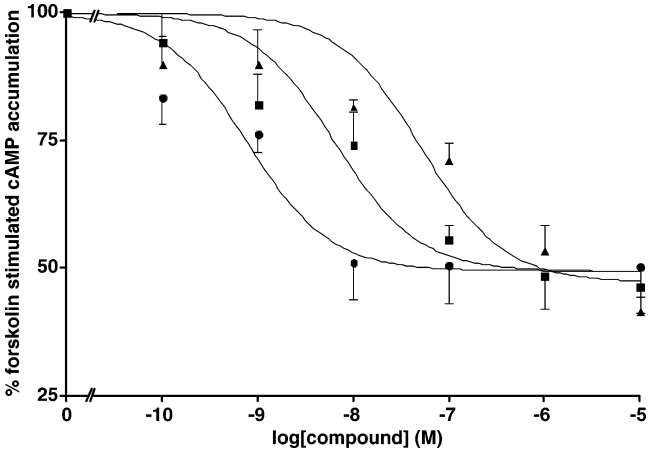

Figure 2. Effect of various concentrations of the sst_1-selective agonists **(20, 34)** in comparison with SRIF-28 as positive control on forskolin-stimulated cAMP accumulation in CHO-K1 cells expressing sst_1. Concentration−response curves were obtained with increasing concentrations of SRIF-28 (●), **34** (■), and **20** (▲). Data are expressed as % forskolin-stimulated cAMP accumulation. The plot represents the mean of three independent experiments in duplicate (mean ± SEM).

phate (cAMP) in sst_1 expressing CCL39 or CHO-K1 cells. Data are shown in Figures 1 and 2, respectively. The agonist SRIF-28, at a peptide concentration of 100 nM, potently inhibited forskolin-stimulated cAMP accumulation by more than 81% in CCL39 transfected cells (EC_{50} = 0.18 nM) and by more than 49% in CHO-K1 transfected cells (EC_{50} = 0.77 nM). SRIF-28 was used as positive control. Analogues tested in these systems, **20** and **34** in CHO-K1 transfected cells and **17**, **19**, and **42** in CCL39 transfected cells, were selected on the basis of unique structural constraints and high-binding affinity in each category. All five compounds showed agonistic properties with EC_{50} values of 5.3 nM for **17**, 2.1 nM for **19**, 1.5 nM for **42**, 6.4 nM for **34**, and 51 nM for **20**. The sst_3-selective sst_3−ODN-8[54] was used as negative control in CCL39 transfected cells and, as expected, behaves as inactive (data not shown).

As mentioned earlier, the aim of this study was to use the available structure−activity relationship (SAR) of sst_1-selective analogues for the design of sst_1-selective antagonists. We hypothesized that structural constraints such as N^{α}-methylation of the backbone could fulfill this aim. SRIF-28 (**1**), Des-Asn^5-[D-Trp^8]SRIF (**2**), Des-Ala^1,Gly^2,Asn^5-[D-Trp^8,IAmp^9]SRIF (**3**), and Des-Ala^1,Gly^2,Asn^5-[D-Nal^8,IAmp^9]SRIF (**4**) in Table 1 are the reference analogues for this study. SRIF-28 (**1**) has high affinity (IC_{50} = 2−4 nM at all sst). Des-Asn^5-[D-Trp^8]SRIF (**2**) is also very potent at all receptors (IC_{50} = 1−5 nM at all sst) except for sst_2 (IC_{50} = 43 nM at sst_2). Des-Ala^1,Gly^2,Asn^5-[D-Trp^8,IAmp^9]SRIF (**3**), the first identified sst_1-selective ligand,[33] was 33 times less potent at sst_1 than its nonselective parent **2** and had some marginal affinity for sst_3 (IC_{50} = 345 nM at sst_3). Substitution of D-Trp^8 by D-Nal^8 further reduced affinity at least 8-fold at all receptors. Despite this loss of affinity (compare affinities of **3** (IC_{50} = 33 nM at sst_1) versus **4** (IC_{50} = 248 nM at sst_1)), we carried out the N^{α}-methyl scan of **4** rather than **3** for practical purposes because our observation was that yields were often lower for the tryptophan-containing analogues, and we did not know which synthetic challenges (described above) we would have to meet to complete our scan (**5**−**15**). Whereas N^{α}-methylation of Lys^4 (**6**), Phe^6 (**7**), Phe^7 (**8**), Thr^{10} (**11**), and Phe^{11} (**12**) resulted in loss of affinity at all receptors, N^{α}-methylation at Cys^3 (**5**), D-Nal^8 (**9**), Thr^{12} (**13**), and Cys^{14} (**15**) was tolerated. Analogues **10** (N^{α}Me-IAmp^9) and **14** (N^{α}Me-Ser^{13}) both showed about 3-fold better binding affinity at sst_1 than **4**. These results are not very different from those of Rajeswaran et al.[42,43] who found similar compatibility (N^{α}-methylation of Lys^9) in a series of antagonists based on a different scaffold. This suggests that selectivity for sst_1 (our data) and other sst (mostly sst_2, sst_3, and sst_5) are less sensitive to backbone configuration than ring size and side chain composition.

With the knowledge that N^{α}-methylation at positions 3, 9, 12, 13, and 14 was compatible with retention of some activity, we introduced this modification in **3** to yield **16**−**20**, respectively. As expected from the observation that **3** is more potent than **4**, analogues **16**−**20** are more potent than the corresponding **5**, **10**, **13**, **14**, and **15** with retention of sst_1 selectivity. In this series, **17** and **19** are the most potent with >20-fold selectivity over all other receptors.

As an intermediate in the synthesis of **19**, we also tested **21**, which has the same sequence extended by two lysine residues at the C-terminus. Unexpectedly, this modification was not deleterious (only 2-fold loss of affinity at sst_1). Similarly, **22** and **23** are the C-terminus extensions of **15** by three and one lysine residues, as are **24** and **25** of **20**. These analogues retained equal or slightly improved affinity to that of their parents. Because C-terminus lysine extensions drastically change the solubility characteristics of these analogues, one can imagine situations whereby such a property can be taken advantage of for formulation purposes, cocrystallization with the cognate receptor or fragment, or to reduce nonspecific binding of a ligand, among others.

The next series of analogues (**26**−**29**) has a tyrosine at position 2. We have already described the properties

of **26**[1] and used it as an sst_1-selective radioligand. N^{α}-methylation of IAmp[9] to yield **27**, carbamoylation of the N-terminus as in **28**, or the combination of both substitutions to yield **29** in order to demonstrate the possible additivity of favorable substitutions first described in a series of sst_3-selective analogues[54] did not significantly influence the binding affinity or selectivity of any of these peptides. Monoiodination of **29** to yield **30** had no significant effect on its affinity.

In the next series, we investigated the effect of N^{α}-methylation on tyrosine-containing analogues at position 11. The properties of the parent peptides **32**, **36**, and **38** have already been described.[1] It is, however, remarkable to see the difference in selectivity (or lack thereof) of **31** versus **32** as the result of the substitution of a Lys^9 by $IAmp^9$ with retention of high affinity at sst_1. N^{α}-methylation of **32** at position 9 without (**34**) or with (**35**) monoiodination of Tyr^{11} did only marginally alter the high affinity or selectivity. Changing the chirality of Trp^8 of **32** from D to L to yield **33** did not affect the binding affinity or selectivity except at sst_4. In the corresponding carbamoylated series (**36**−**39**), we had already identified the most potent and sst_1-selective analogues **36** and **38**; their N^{α}-methylation at position 9 to yield **37** and **39** had no significant effect on affinity at sst_1. Clearly, it was more advantageous to introduce a tyrosine for the purpose of iodination at position 11 rather than at position 2 in sst_1-selective analogues.

Two analogues with D-Nal^8 (**40** and **41**) to be compared with the D-Trp^8-containing **34** and **37** again showed an approximate 4-fold loss in affinity for sst_1. Because these analogues were so potent at sst_1 and impotent at the other four receptors, a few fold difference in affinity at sst_1 could not infer increases or losses in selectivity.

Finally, we investigated the effect of N^{β}-methylation of Agl^8-containing (Agl = aminoglycine) sst_1-selective analogues. We had shown that a substituted Agl at position 8 in an octapeptide had resulted in a potent sst_3-selective antagonist[54] and were expecting this substitution to yield an sst_1-selective antagonist. Whereas **43** containing the L-isomer at position 8 was inactive at the doses tested, the corresponding **42** containing the D-isomer at position 8 was among the most potent and sst_1-selective agonists, suggesting that the indol-3-carbonyl derivative versus the 2-naphthoyl analogue would be much more potent. As published earlier,[55] we had extreme difficulties in coupling indole-3-carboxylic acid to N^{β}Me-Agl in a TRH analogue. It is noteworthy that the monoiodinated **44** and **45**, although retaining high sst_1-binding affinity, lose some selectivity toward sst_3 and sst_4.

In conclusion, when comparing the affinities of **2** to that of SRIF-14 (IC_{50} values = 1.9 ± 0.53 (5); 0.7 ± 0.2 (5); 3.3 ± 1.7 (4); 1.6 ± 0.8 (4); 10 ± 4.4 (4) nM at the five sst, respectively, number of assays in parentheses), we can now hypothesize that the loss of affinity for sst_2 (ca. 60-fold) was due to a conformational change of the SRIF ring (contraction of a 12 amino acid ring down to 11) resulting from the deletion of Asn^5. The loss of affinity of **3** for receptors sst_{2-5} as compared to **2** resulted from the introduction of IAmp at position 9 in lieu of Lys because we know that deletion of residues 1 and 2 in SRIF has no influence on either affinity or selectivity.[1] We have shown that in the octapeptide Des-$AA^{1,2,4,5,12,13}$-SRIF loss of affinity for all receptors except sst_4 can be achieved by substituting Phe^7 by Ala^7.[39] In the same octapeptide, substitution of Trp^8 by D-Agl^8(N^{β}-Me,2-naphthoyl) leads to both sst_3 selectivity and antagonistic activity. Here, we demonstrate that N^{α}-methylation of residues 9 (**17**, **34**), 13 (**19**), and 14 (**20**) is compatible with significant binding affinity without influencing the ability of these compounds to activate their cognate receptor.

Experimental Procedures

Starting Materials. The Boc-Cys(Mob)-CM resin with a capacity of 0.3−0.5 mequiv/g was obtained according to published procedures (Mob = 4-methoxybenzyl).[56] All N^{α}-*tert*-butoxycarbonyl (Boc) protected amino acids with side chain protection were purchased from Bachem Inc. (Torrance, CA), Chem-Impex Intl. (Wood Dale, IL), Novabiochem (San Diego, CA), or Reanal (Budapest, Hungary). The side chain protecting groups were as follows: Cys(Mob), Lys[Z(2Cl)] Ser(Bzl), Thr(Bzl), Tyr[Z(2Br)], and m-I-Tyr[Bzl(3Br)]. Boc-IAmp(Z),[57] Boc-N^{α}Me-IAmp(Z), Fmoc-D/L-Agl(N^{β}Me,Boc),[58] and Fmoc-D-Agl(Boc)[59] were synthesized in our laboratory (Bzl = benzyl, (Bzl)3Br = 3-bromobenzyl, Z(2Br) = 2-bromobenzyloxycarbonyl, Z(2Cl) = 2-chlorobenzyloxycarbonyl, Fmoc = 9-fluorenylmethoxycarbonyl. All N^{α}-methylated amino acids were obtained on the resin as described in the literature.[46] Carboxypeptidase B was purchased from Roche Molecular Biochemicals (U.S.A.). All of the reagents and solvents were reagent grade or better and used without further purification.

Peptide Synthesis. Peptides were synthesized by the solid-phase approach with Boc chemistry either manually or on a CS-Bio Peptide Synthesizer model CS536. Boc-Cys(Mob)-CM resin with a capacity of 0.3−0.5 mequiv/g was used. Couplings of the protected amino acids were mediated by diisopropylcarbodiimide (DIC) in CH_2Cl_2 or *N*-methylpyrrolidinone (NMP) for 1 h and monitored by the qualitative ninhydrin test.[60] A 3-equiv excess of the protected amino acids based on the original substitution of the resin was used in most cases. Boc removal was achieved with trifluoroacetic acid (60% in CH_2Cl_2, 1−2% ethanedithiol, or *m*-cresol) for 20 min. An isopropyl alcohol (1% *m*-cresol) wash followed trifluoroacetic acid (TFA) treatment, and then successive washes with triethylamine solution (10% in CH_2Cl_2), methanol, triethylamine solution, methanol, and CH_2Cl_2 completed the neutralization sequence.

N^{α}-Methylation of Peptides 5−13 and 16−18 (Table 1). The N^{α}-methylamino group was formed on the resin as described in the literature.[46] After the amino group at the desired methylation site was deblocked with TFA (60% in CH_2Cl_2, 1% *m*-cresol), the freed and neutralized amino function was alkylated by shaking the resin with 4 equiv of Dod-Cl (4,4′-dimethoxyditYl chloride) and 4 equiv of diisopropylethylamine (DIPEA) in CH_2Cl_2 for 1 h. The resin was washed with CH_2Cl_2, triethylamine solution (10% in CH_2Cl_2), methanol, and CH_2Cl_2. A formalin solution (37%, 8 mL) and 0.15 mL of acetic acid in NMP (15 mL) were added to the resin, the mixture was shaken for 5 min followed by the addition of sodium cyanoborohydride (350 mg) to the reaction mixture, and that mixture was shaken for an additional half hour. The resin was washed with CH_2Cl_2, and for completeness of the reaction, the reductive methylation was repeated. The removal of the Dod group with TFA (60%) permitted the solid-phase synthesis to proceed. This approach was used for the synthesis of all of the N^{α}-methylated analogues in Table 1, except **15**, **19**−**25**.

N^{α}-Methylation of Peptides 15 and 19−25 (Table 1). We were unable to methylate Cys^{14} with the method of Kaljuste[46] described above, and N^{α}-methylation of serine at position 13 in analogue **14** resulted in a very low yield. For the synthesis of **15**, we tried to use *o*-nitrobenzenesulfonyl chloride (3 equiv) and collidine (3 equiv) in CH_2Cl_2 to protect the N-terminus of the resin bound Cys and then selectively deprotonate the amide N−H of *o*-nitrobenzenesulfonamide by the nonionic base

MTBD (1,3,4,6,7,8-hexahydro-1-methyl-2H-pyrimido[1,2-a]-pyrimidine) (3 equiv) and methylate with dimethyl sulfate (3 equiv) in DMF as described by Miller et al.,[47] but this method did not result in the methylated product. Therefore, to perform N^{α}-methylation of Ser[13] and Cys[14] by the method of Kaljuste in analogues **19**, **15**, and **20**, we extended their C terminal by Lys-Lys and Lys-Lys-Lys, respectively (**21**, **22**, and **24**).

Enzymatic Hydrolysis of the Lys-Extended Analogues (21, 22, and 24). Peptides (**21**, **22**, **24**) were cleaved from the resin by HF and purified on preparative HPLC, followed by the hydrolysis of the C-terminal $(Lys)_2$ and $(Lys)_3$ extensions with carboxypeptidase B, which resulted in the target peptides (**19**, **15**, and **20**). Peptide **21** (25 μM) was hydrolyzed in 0.1 M NaCl/0.05M Tris buffer at pH 7.6 (150 mL) with undiluted carboxypeptidase B enzyme solution (75U, 100 μL) at room temperature. The hydrolysis was complete in 20 min, resulting in analogue **19** (Table 1). The product was desalted by preparative RP-HPLC and pure **19** (14.7 μM) was obtained (yield of hydrolysis, 59%). Peptide **22** (15 μM) was hydrolyzed in 0.1 M NaCl/0.05 M Tris buffer at pH 7.6 (40 mL) with undiluted carboxypeptidase B enzyme solution (56.25U, 75 μL) at room temperature for 24 h. The reaction was stopped with 0.1 N HCl (4 mL). According to analytical RP-HPLC, 20% of the hydrolyzate showed a peptide extended still with one Lys, and 80% of the product was the desired one. The two peptides were separated by preparative RP-HPLC. Yields of **15** and **23** (Table 1) were 8.2 and 3.2 μM, respectively (76%). Peptide **24** (4 μM) was hydrolyzed in 0.1 M NaCl/0.05 M Tris buffer at pH 7.6 (15 mL) with undiluted carboxypeptidase B enzyme solution (37.5U, 50 μL) at room temperature for 30 min followed by a second addition of the enzyme (50 μL); the hydrolysis was continued for an additional 5 h. The reaction was stopped with 0.1 N HCl (1.5 mL). According to analytical RP-HPLC, half of the hydrolyzate showed a peptide extended still with one Lys and the other half of the product was the desired one. The two peptides were separated by preparative RP-HPLC. Analogues **20** (2 μM) and **25** (1.7 μM) (Table 1) were obtained (yield of hydrolysis, 92%).

Synthesis of Peptides Containing N^{α}Me-IAmp in Position 9 (34, 35, 37, and 39−41). Synthesis of Boc-N^{α}Me-IAmp(Z)-OH. Sodium hydride (1 g, 60% dispersion in oil, 25 mmol) was added to a cooled solution of Boc-IAmp(Z)[57] in tetrahydrofuran (25 mL) and stirred at 0 °C for 1 h when MeI (0.7 mL, 11 mmol) in tetrahydrofuran (4 mL) was added to the reaction mixture and it was stirred at 22 °C overnight. The reaction was followed by analytical HPLC (Vydac C18 column, 1.5 mL/min flow rate, isocratic elution with 78% B solvent (B: 60% acetonitrile, 40% water, 0.1% TFA; A: 0.1% TFA in water)). The N^{α}-methylated amino acid derivative eluted 2 min later than the starting material at 12.5 min. The excess reagents were quenched with EtOH and water. After removal of the solvents in vacuo, the residue was dissolved in EtOAc/water = 1:1 (100 mL), and the reaction mixture was adjusted to pH 3 with citric acid solution (0.25 N). The aqueous phase was separated and extracted with EtOAc (2 × 50 mL). All EtOAc extracts were combined and dried over anhydrous $MgSO_4$. The dried EtOAc solution was evaporated in vacuo and resulted in 2 g (82%) of Boc-N^{α}Me-IAmp(Z)-OH as a thick oil. MALDI/MS *m/e* obsd: 484.92 (M + H). Calcd: 485.27(M + H). Boc-N^{α}Me-IAmp(Z)-OH was used in the solid-phase synthesis of **27**, **29**, **30**, **34**, **35**, **37**, and **39**−**41**.

Carbamoylation of Peptides 28−30, 37−39, and 41. The ureido group (Cbm) at the N terminus of **28**−**30, 37**−**39**, and **41** was introduced on the resin (Cbm = carbamoyl). The N-terminal Boc group of the fully assembled peptide was deprotected with 60% TFA in CH_2Cl_2 and neutralized with 10% triethylamine (TEA) in CH_2Cl_2. Then carbamoylation with NaOCN (100 mg, 0.65 mmol) in NMP (4 mL) and glacial acetic acid (3 mL per gram of initial resin) proceeded. The mixture was agitated at room temperature for 30 min, and the ninhydrin test indicated a complete reaction.

Synthesis of Peptides 42−45 (Table 1). First, the two Agl-containing peptides (**42, 43**) were synthesized using unresolved Fmoc-D/L-Agl(N^{β}Me,Boc).[58] After the removal of the Boc group with TFA, 3 equiv of naphthoyl chloride and 3 equiv of DIPEA were used to acylate the free secondary amino group of the side chain. Removal of the N^{α}-Fmoc protecting group with 20% piperidine in NMP in two successive 5 and 15 min treatments was followed by the standard elongation protocol until the completion of the peptide. To be able to assign the stereochemistry of Agl in analogues **42** and **43**, the same sequence was also synthesized starting with resolved Fmoc-D-Agl(Boc)-OH,[59] and the N^{β}Me group was formed on the resin with the Kaljuste method as described above.[46]

Peptide Cleavage, Deprotection, and Cyclization. All peptides were cleaved from the resin support with simultaneous side chain deprotection by anhydrous HF containing the scavengers anisole (10% v/v) and methyl sulfide (5% v/v) for 60 min at 0 °C. The diethyl ether precipitated crude peptides were cyclized in 75% acetic acid (200 mL) by addition of iodine (10% solution in methanol) until the appearance of a stable orange color. After 40 min, ascorbic acid was added to quench the excess iodine.

Purification and Characterization of the Analogues. The crude, lyophilized peptides were purified by preparative RP-HPLC[50] on a 5 × 30 cm cartridge, packed in the laboratory with reversed-phase 300 Å Vydac C_{18} silica (15−20 μm particle size) using a Waters Associates (Milford, MA) DeltaPrep 3000 System and model Shimadzu SPD-6A variable wavelength UV detector, Huston Instruments Omni Scribe chart recorder. The peptides eluted with a flow rate of 100 mL/min using a linear gradient of 1% B per 3 min increase from the baseline % B. (Eluent A = 0.25 N triethylammonium phosphate (TEAP) pH 2.25, eluent B = 60% CH_3CN, 40% A.) As a final step, all peptides were rechromatographed in a 0.1% TFA solution and acetonitrile on the same cartridge at 100 mL/min (gradient of 1% acetonitrile/min). Analytical RP-HPLC screening was performed on a Vydac C_{18} column (0.46 × 25 cm, 5 μm particle size, 300 Å pore size) connected to a Rheodyne model 7125 injector, an Altex 420 HPLC system using two Altex 100A pumps, a Kratos Spectroflow 757 UV detector set to 210 nm, and a Houston Instruments D-5000 strip chart recorder. The fractions containing the product were pooled and subjected to lyophilization. The diastereomers **42** and **43** could be separated by preparative RP-HPLC. The same peptide sequence synthesized with the papain-resolved, optically active D-Agl,[59] and N^{β}-methylated on the resin[46] coeluted with the later eluting diastereomer **43,** which was obtained by the RP-HPLC separation of the product synthesized with the unresolved Agl derivative.

The purity of the final peptides were determined by analytical RP-HPLC performed with a linear gradient using 0.1 M TEAP pH 2.5 as eluent A and 60% CH_3CN/40% A as eluent B on a Hewlett-Packard Series II 1090 liquid chromatograph connected to a Vydac C_{18} column (0.21 cm × 15 cm, 5 μm particle size, 300 Å pore size), controller model 362, and a Think Jet printer. Capillary zone electrophoresis (CZE) analysis was performed on a Beckman P/ACE System 2050 controlled by an IBM Personal System/2 model 50Z connected to a ChromJet integrator.[51] Peptides were greater than 90% pure by HPLC and CZE in most cases. Mass spectra (MALDI-TOF-MS) were measured on an ABI−Perseptive DE-STR instrument. The instrument employs a nitrogen laser (337 nm) at a repetition rate of 20 Hz. The applied accelerating voltage was 20 kV. Spectra were recorded in delayed extraction mode (300 ns delay). All of the spectra were recorded in the positive reflector mode. Spectra were sums of 100 laser shots. Matrix α-cyano-4-hydroxycinnamic acid was prepared as saturated solutions in 0.3% trifluoroacetic acid in 50% acetonitrile. The observed monoisotopic $(M + H)^+$ values of each peptide corresponded with the calculated $(M + H)^+$ values (Table 1).

Cell Culture. CHO-K1 cells stably expressing human sst_1 and sst_5 were kindly provided by Drs. T. Reisine and G. Singh (University of Pennsylvania, Philadelphia, PA) and CCL39 cells stably expressing human sst_1, sst_2, sst_3, and sst_4 by Dr. D. Hoyer (Novartis Pharma, Basel, Switzerland). Cells were grown as described previously.[52] All culture reagents were supplied by Gibco BRL, Life Technologies (Grand Island, NY).

Receptor Autoradiography. Cell membrane pellets were prepared and receptor autoradiography was performed as depicted in detail previously.[52]

Binding studies were performed as reported previously[52] with [Leu^8,D-Trp^{22},^{125}I-Tyr^{25}]-SRIF-28 on cell pellet sections and on tissue sections of sst_1-expressing human tumors using 15 000 cpm/100 μL of the radioligand.

Adenylate Cyclase Activity. Modulation of forskolin-stimulated adenylate cyclase activity was determined using a radioimmunoassay measuring intracellular cAMP levels by competition binding. Cells expressing sst_1 (CHO-K1 for **20** and **34**, and CCL39 for **17**, **19**, and **42**) were subcultured either in 96-well culture plates (CHO-K1 transfected cells) or in poly-D-lysine-coated 96-well culture plates (CCL39 transfected cells) at 2×10^4 cells/well and grown for 24 h. Culture medium was removed from the wells and 100 μL of fresh medium containing 0.5 mM 3-isobutyl-I-methylxanthine (IBMX) was added to each well. Cells were incubated for 30 min at 37 °C. Medium was then removed and replaced with 100 μL of fresh medium containing 0.5 mM IBMX, with or without 3 μM forskolin (CHO-K1 transfected cells) or 7.5 μM forskolin (CCL39 transfected cells) and various concentrations of the compounds to be tested. Cells were incubated for 30 min at 37 °C. After removal of medium, cells were lysed, and cAMP accumulation was determined using a commercially available cAMP scintillation proximity assay (SPA) system, according to the instructions of the manufacturer (RPA 538, Amersham Biosciences, Little Chalfont, U.K.). Data for cAMP were expressed as percentage of stimulation over the nonstimulated level. Values of EC_{50} (the agonist concentration causing 50% of its maximal effect) were derived from concentration−response curves.

Acknowledgment. This work was supported in part by NIH Grant RO1 DK 59953. The authors thank Dr. T. Reisine for the generous gift of sst transfected cells. We are indebted to D. Kirby, R. Kaiser, C. Miller, and T. Goedken for technical assistance in the synthesis and characterization of the peptides and Drs. W. Fisher and A. G. Craig for mass spectrometric analysis of the analogues. J.R. is the Dr. Frederik Paulsen Chair in Neurosciences Professor.

References

(1) Rivier, J. E.; Hoeger, C.; Erchegyi, J.; Gulyas, J.; DeBoard, R.; et al. Potent somatostatin undecapeptide agonists selective for somatostatin receptor 1 (sst_1). *J. Med. Chem.* **2001**, *44*, 2238−2246.

(2) Erchegyi, J.; Hoeger, C.; Wenger, S.; Waser, B.; Schaer, J.-C. et al. *N*-methyl scan of a sst_1-selective somatostatin (SRIF) analog. *Peptides − The wave of the future: 2nd International Peptide Symposium/17th American Peptide Symposium*; American Peptide Symposium: San Diego, CA, 2001; pp 719−720.

(3) Brazeau, P.; Vale, W. W.; Burgus, R.; Ling, N.; Butcher, M. et al. Hypothalamic polypeptide that inhibits the secretion of immunoreactive pituitary growth hormone. *Science* **1973**, *179*, 77−79.

(4) Guillemin, R.; Gerich, J. E. Somatostatin: physiological and clinical significance. *Annu. Rev. Med.* **1976**, *27*, 379−388.

(5) Meyerhof, W.; Paust, H. J.; Schoenrock, C.; Richter, D. Cloning of a cDNA encoding a novel putative G-protein-coupled receptor expressed in specific rat brain regions. *DNA Cell Biol.* **1991**, *10*, 689−694.

(6) Meyerhof, W.; Wulfsen, I.; Schönrock, C.; Fehr, S.; Richter, D. Molecular cloning of a somatostatin-28 receptor and comparison of its expression pattern with that of a somatostatin-14 receptor in rat brain. *Proc. Natl. Acad. Sci. U.S.A.* **1992**, *89*, 10267−10271.

(7) Bruno, J. F.; Xu, Y.; Song, J.; Berelowitz, M. Molecular cloning and functional expression of a brain-specific somatostatin receptor. *Proc. Natl. Acad. Sci. U.S.A.* **1992**, *89*, 11151−11155.

(8) Rohrer, L.; Raulf, F.; Bruns, C.; Buettner, R.; Hofstaedter, F. et al. Cloning and characterization of a fourth human somatostatin receptor. *Proc. Natl. Acad. Sci. U.S.A.* **1993**, *90*, 4196−4200.

(9) Xu, Y.; Song, H.; Bruno, J. F.; Berelowitz, M. Molecular cloning and sequencing of a human somatostatin receptor, hSSTR4. *Biochem. Biophys. Res. Commun.* **1993**, *193*, 648−652.

(10) Yamada, Y.; Post, S. R.; Wang, K.; Medical, H.; Tager, S. et al. Cloning and functional characterization of a family of human and mouse somatostatin receptors expressed in brain, gastrointestinal tract, and kidney. *Proc. Natl. Acad. Sci. U.S.A.* **1992**, *89*, 251−255.

(11) Yamada, Y.; Kagimoto, S.; Kubota, A.; Yasuda, K.; Masuda, K. et al. Cloning, functional expression and pharmacological characterization of a fourth (hSSTR4) and fifth (hSSTR5) human somatostatin receptor subtype. *Biochem. Biophys. Res. Commun.* **1993**, *195*, 844−852.

(12) Siehler, S.; Hoyer, D. Characterisation of human recombinant somatostatin receptors. 4. Modulation of phospholipase C activity. *Naunyn-Schmiedeberg's Arch Pharmacol.* **1999**, *360*, 522−532.

(13) Hannon, J. P.; Nunn, C.; Stolz, B.; Bruns, C.; Weckbecker, G. et al. Drug design at peptide receptors: somatostatin receptor ligands. *J. Mol. Neurosci.* **2002**, *18*, 15−27.

(14) Katz, M. D.; Erstad, B. L. Octreotide, a new somatostatin analogue. *Clin. Pharm.* **1989**, *8*, 255−273.

(15) Raynor, K.; Murphy, W.; Coy, D.; Taylor, J.; Moreau, J. P. et al. Cloned somatostatin receptors: Identification of subtype selective peptides and demonstration of high affinity binding of linear peptides. *Mol. Pharmacol.* **1993**, *43*, 838−844.

(16) Raynor, K.; OCarroll, A.-M.; Kong, H.; Yasuda, K.; Mahan, L. et al. Characterization of the cloned somatostatin receptors SSTR4 and SSTR5. *Mol. Pharmacol.* **1993**, *44*, 385−392.

(17) Patel, Y. C. Somatostatin and its receptor family. *Front. Neuroendocrinol.* **1999**, *20*, 157−198.

(18) Piwko, C.; Thoss, V. S.; Schupbach, E.; Kummer, J.; Langenegger, D. et al. Pharmacological characterisation of human cerebral cortex somatostatin SRIF1 and SRIF2 receptors. *Naunyn Schmiedebergs Arch Pharmacol.* **1997**, *355*, 161−167.

(19) Reubi, J. C.; Schaer, J. C.; Waser, B.; Hoeger, C.; Rivier, J. A selective analogue for the somatostatin sst1-receptor subtype expressed by human tumors. *Eur. J. Pharmacol.* **1998**, *345*, 103−110.

(20) Albers, A. R.; O'Dorisio, M. S.; Balster, D. A.; Caprara, M.; Gosh, P. et al. Somatostatin receptor gene expression in neuroblastoma. *Regul. Peptides* **2000**, *88*, 61−73.

(21) Pawlikowski, M.; Pisarek, H.; Kunert-Radek, J.; Radek, A. Immunohistochemical detection of somatostatin receptor subtypes in "clinically nonfunctioning" pituitary adenomas. *Endocr. Pathol.* **2003**, *14*, 231−238.

(22) Schulz, S.; Schmitt, J.; Weise, W. Frequent expression of immunoreactive somatostatin receptors in cervical and endometrial cancer. *Gynecol. Oncol.* **2003**, *89*, 385−390.

(23) Thermos, K. Functional mapping of somatostatin receptors in the retina: a review. *Vision Res.* **2003**, *43*, 1805−1815.

(24) Mawrin, C.; Schulz, S.; Pauli, S. U.; Treuheit, T.; Diete, S. et al. Differential expression of sst1, sst2A, and sst3 somatostatin receptor proteins in low-grade and high-grade astrocytomas. *J. Neuropathol. Exp. Neurol.* **2004**, *63*, 13−19.

(25) Olias, G.; Viollet, C.; Kusserow, H.; Epelbaum, J.; Meyerhof, W. Regulation and function of somatostatin receptors. *J. Neurochem.* **2004**, *89*, 1057−1091.

(26) Lanneau, C.; Bluet-Pajot, M. T.; Zizzari, P.; Csaba, Z.; Dournaud, P. et al. Involvement of the Sst1 somatostatin receptor subtype in the intrahypothalamic neuronal network regulating growth hormone secretion: an in vitro and in vivo antisense study. *Endocrinology* **2000**, *141*, 967−979.

(27) Zhang, W. H.; Beaudet, A.; Tannenbaum, G. S. Sexually dimorphic expression of sst1 and sst2 somatostatin receptor subtypes in the arcuate nucleus and anterior pituitary of adult rats. *J. Neuroendocrinol.* **1999**, *11*, 129−136.

(28) Zatelli, M. C.; Piccin, D.; Tagliati, F.; Ambrosio, M. R.; Margutti, A.; et al. Somatostatin receptor subtype 1 selective activation in human growth hormone (GH)- and prolactin (PRL)-secreting pituitary adenomas: effects on cell viability, GH, and PRL secretion. *J. Clin. Endocrinol. Metab.* **2003**, *88*, 2797−2802.

(29) Vasilaki, A.; Papasava, D.; Hoyer, D.; Thermos, K. The somatostatin receptor (sst(1)) modulates the release of somatostatin in the nucleus accumbens of the rat. *Neuropharmacology* **2004**, *47*, 612−618.

(30) Hoyer, D.; Dixon, K.; Gentsch, C.; Vassout, A.; Enz, A. et al. NVP−SRA880, a somatostatin sst_1 receptor antagonist promotes social interactions, reduces aggressive behaviour and stimulates learning. *The Pharmacologist* **2002**, *44*, A254.

(31) Hoyer, D.; Nunn, C.; Hannon, J.; Schoeffter, P.; Feuerbach, D. et al. SRA880, in vitro characterization of the first non-peptide somatostatin sst_1 receptor antagonist. *Neurosci. Lett.* **2004**, *361*, 132−135.

(32) Ösapay, G.; Ösapay, K. Therapeutic applications of somatostatin analogues. *Expert Opin. Ther. Patents* **1998**, *8*, 855−870.

(33) Liapakis, G.; Hoeger, C.; Rivier, J.; Reisine, T. Development of a selective agonist at the somatostatin receptor subtype SSTR1. *J. Pharmacol. Exp. Ther.* **1996**, *276*, 1089−1094.

(34) Rivier, J.; Brown, M.; Vale, W. [D-Trp[8]]-somatostatin: An analogue of somatostatin more potent than the native molecule. *Biochem. Biophys. Res. Commun.* **1975**, *65*, 746−751.
(35) Bauer, W.; Briner, U.; Doepfner, W.; Haller, R.; Huguenin, R. et al. SMS 201−995: a very potent and selective octapeptide analogue of somatostatin with prolonged action. *Life Sci.* **1982**, *31*, 1133−1140.
(36) Veber, D. F.; Freidinger, R. M.; Perlow, D. S.; Paleveda, W. J., Jr.; Holly, F. W. et al. A potent cyclic hexapeptide analogue of somatostatin. *Nature* **1981**, *292*, 55−58.
(37) Meyers, C. A.; Coy, D. H.; Huang, W. Y.; Schally, A. V.; Redding, T. W. Highly active position eight analogues of somatostatin and separation of peptide diastereomers by partition chromatography. *Biochemistry* **1978**, *17*, 2326−2330.
(38) Rivier, J.; Erchegyi, J.; Hoeger, C.; Miller, C.; Low, W. et al. Novel sst_4-selective somatostatin (SRIF) agonists. Part I: Lead identification using a betide scan. *J. Med. Chem.* **2003**, *46*, 5579−5586.
(39) Erchegyi, J.; Waser, B.; Schaer, J.-C.; Cescato, R.; Brazeau, J. F. et al. Novel sst_4-selective somatostatin (SRIF) agonists. Part III: Analogues amenable to radiolabeling. *J. Med. Chem.* **2003**, *46*, 5597−5605.
(40) Reubi, J. C.; Schaer, J.-C.; Waser, B.; Hoeger, C.; Rivier, J. A selective analogue for the somatostatin sst1-receptor subtype expressed by human tumors. *Eur. J. Pharmacol.* **1998**, *345*, 103−110.
(41) Rohrer, S. P.; Birzin, E. T.; Mosley, R. T.; Berk, S. C.; Hutchins, S. M. et al. Rapid identification of subtype-selective agonists of the somatostatin receptor through combinatorial chemistry. *Science* **1998**, *282*, 737−740.
(42) Rajeswaran, W. G.; Hocart, S. J.; Murphy, W. A.; Taylor, J. E.; Coy, D. H. *N*-methyl scan of somatostatin octapeptide agonists produces interesting effects on receptor subtype specificity. *J. Med. Chem.* **2001**, *44*, 1416−1421.
(43) Rajeswaran, W. G.; Hocart, S. J.; Murphy, W. A.; Taylor, J. E.; Coy, D. H. Highly potent and subtype selective ligands derived by *N*-methyl scan of a somatostatin antagonist. *J. Med. Chem.* **2001**, *44*, 1305−1311.
(44) Rivier, J.; Kirby, D.; Erchegyi, J.; Waser, B.; Eltschinger, V. et al. Somatostatin receptor 1 selective analogues: 3. Dicyclic peptides. *J. Med. Chem.* **2005**, *48*, 515−522.
(45) Grace, C. R. R.; Durrer, L.; Koerber, S. C.; Erchegyi, J.; Reubi, J. C. et al. Somatostatin receptor 1 selective analogues: 4. Three-dimensional consensus structure by NMR. *J. Med. Chem.* **2005**, *48*, 523−533.
(46) Kaljuste, K.; Undén, A. New method for the synthesis of *N*-methyl amino acids containing peptides by reductive methylation of amino groups on the solid phase. *Int. J. Pept. Prot. Res.* **1993**, *42*, 118−124.
(47) Miller, S. C.; Scanlan, T. S. Site-selective N-methylation of peptides on solid support. *J. Am. Chem. Soc.* **1997**, *119*, 2301−2302.
(48) Ambler, R. P. *Methods in Enzymology*; Academic Press: New York, 1967; p 437.
(49) Rivier, J.; Kaiser, R.; Galyean, R. Solid-phase synthesis of somatostatin and glucagon selective analogues. *Biopolymers* **1978**, *17*, 1927−1938.
(50) Miller, C.; Rivier, J. Peptide chemistry: Development of high-performance liquid chromatography and capillary zone electrophoresis. *Biopolymers* **1996**, *40*, 265−317.
(51) Miller, C.; Rivier, J. Analysis of synthetic peptides by capillary zone electrophoresis in organic/aqueous buffers. *J. Pept. Res.* **1998**, *51*, 444−451.
(52) Reubi, J. C.; Schaer, J. C.; Waser, B.; Wenger, S.; Heppeler, A.; et al. Affinity profiles for human somatostatin receptor sst1-sst5 of somatostatin radiotracers selected for scintigraphic and radiotherapeutic use. *Eur. J. Nucl. Med.* **2000**, *27*, 273−282.
(53) Reubi, J. C. In vitro identification of vasoactive intestinal peptide receptors in human tumors: Implications for tumor imaging. *J. Nucl. Med.* **1995**, *36*, 1846−1853.
(54) Reubi, J. C.; Schaer, J.-C.; Wenger, S.; Hoeger, C.; Erchegyi, J.; et al. Sst_3-selective potent peptidic somatostatin receptor antagonists. *Proc. Natl. Acad. Sci. U.S.A.* **2000**, *97*, 13973−13978.
(55) Kirby, D. A.; Wang, W.; Gershengorn, M. C.; Rivier, J. E. Analogues of thyrotropin-releasing hormone using an aminoglycine based template. *Peptides* **1998**, *19*, 1679−1683.
(56) Horiki, K.; Igano, K.; Inouye, K. Amino acids and peptides. Part 6. Synthesis of the Merrifield resin esters of N-protected amino acids with the aid of hydrogen bonding. *Chem. Lett.* **1978**, *2*, 165−168.
(57) Rivier, J. E.; Jiang, G.; Porter, J.; Hoeger, C.; Craig, A. G.; et al. GnRH antagonists: novel members of the azaline B family. *J. Med. Chem.* **1995**, *38*, 2649−2662.
(58) Jiang, G.-C.; Simon, L.; Rivier, J. E. Orthogonally protected *N*-methyl-substituted α-aminoglycines. *Prot. Pep. Lett.* **1996**, *3*, 219−224.
(59) Sypniewski, M.; Penke, B.; Simon, L.; Rivier, J. (R)-tert-Butoxycarbonylamino-fluorenylmethoxycarbonyl-glycine from (S)-Benzyloxycarbonyl-serine or from papain resolution of the corresponding amide or methyl ester. *J. Org. Chem.* **2000**, *65*, 6595−6600.
(60) Kaiser, E.; Colescott, R. L.; Bossinger, C. D.; Cook, P. I. Color test for detection of free terminal amino groups in the solid-phase synthesis of peptides. *Anal. Biochem.* **1970**, *34*, 595−598.

JM049520L